

Spectroscopy results from CMS



Outline

-Observation of new structure in the $J/\psi J/\psi$ mass spectrum in proton-proton collisions at 13 TeV

-Observation of the $\Lambda_b^0 \rightarrow J/\psi \Xi^- K^+$ decay

-Observation of the rare decay of the η meson to four muons

Jhovanny Andres Mejia Guisao
On behalf of the CMS collaboration

QWG 2024 : The 16th International Workshop on Heavy Quarkonium. 26 February 2024 to 1 March 2024. IISER Mohali.

arXiv:2306.07164,

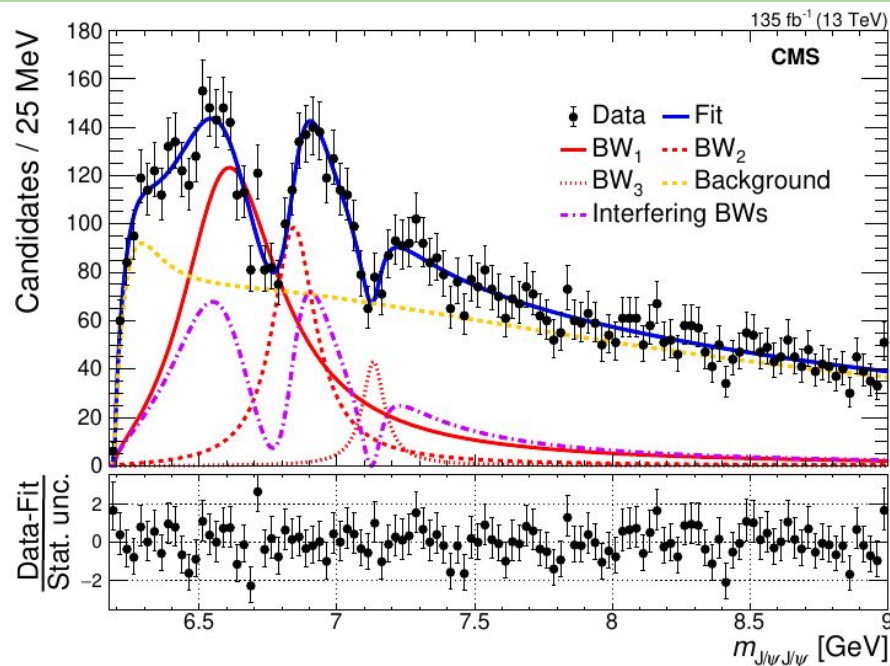
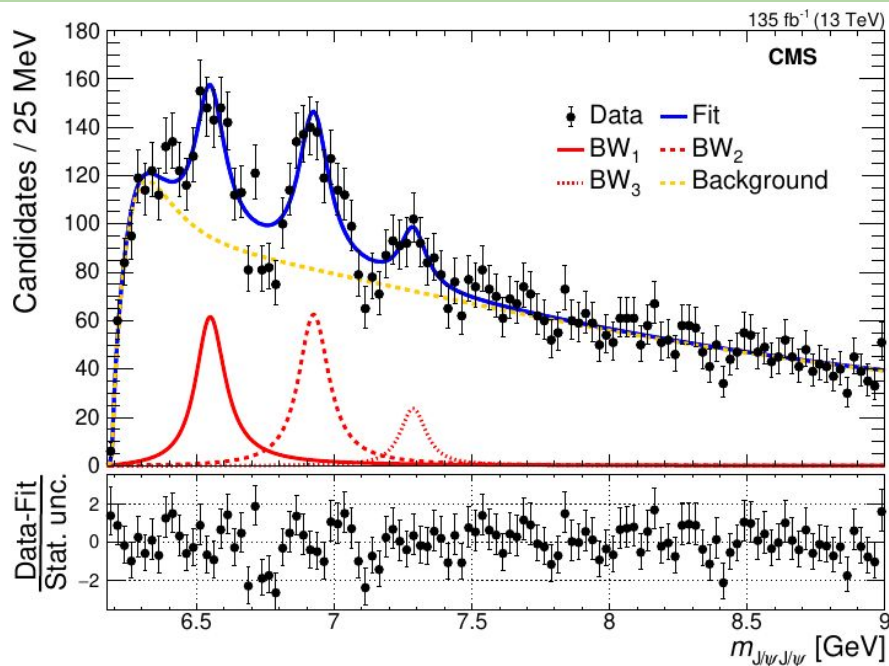
CMS-BPH-21-003 ; CERN-EP-2023-109

Accepted for publication in Phys. Rev. Lett.

Observation of new structure in the $J/\psi J/\psi$ mass spectrum in proton-proton collisions at 13 TeV

While many tetraquark candidates containing heavy quarks are now known, questions still abound, including which of these are truly exotic hadrons, and if they are bound states, what is their internal structure (e.g., molecules, bound states of diquarks, etc).

The $J/\psi J/\psi$ invariant mass spectrum in the range up to 9 GeV



(Left) Fit without interference.

(Right) Fit that includes interference,

Only the sum of the three background components (NRSPS+DPS+BW0) is shown.

The lower portion of the plots shows the pulls.

Summary fit results and dominant contributions to the systematic uncertainties

The "Total uncertainty" is the quadratic sum of all individual components, including the unlisted non-dominant contributions.

Fit	Dominant sources	M_{BW_1}	M_{BW_2}	M_{BW_3}	Γ_{BW_1}	Γ_{BW_2}	Γ_{BW_3}
No-interference	Signal shape	3	3	3	10	5	5
	NRSPS shape	3	1	1	18	15	17
	Feed-down	11	1	1	25	8	6
	Total uncertainty	12	4	5	33	18	19
Interference	Signal shape	7	12	7	56	8	7
	DPS shape	1	3	2	18	6	2
	NRSPS shape	9	14	13	85	9	20
	Mass resolution	8	4	1	24	7	13
	Combinatorial bkg.	7	2	<1	5	3	2
	Feed-down	+0 -27	+44 -0	+38 -0	+0 -210	+19 -0	+12 -0
	Total uncertainty	+16 -31	+48 -20	+41 -15	+110 -240	+25 -17	+29 -26

		BW_1	BW_2	BW_3
No-interference	m [MeV]	$6552 \pm 10 \pm 12$	$6927 \pm 9 \pm 4$	$7287^{+20}_{-18} \pm 5$
	Γ [MeV]	$124^{+32}_{-26} \pm 33$	$122^{+24}_{-21} \pm 18$	$95^{+59}_{-40} \pm 19$
	N	470^{+120}_{-110}	492^{+78}_{-73}	156^{+64}_{-51}
Interference	m [MeV]	6638^{+43+16}_{-38-31}	6847^{+44+48}_{-28-20}	7134^{+48+41}_{-25-15}
	Γ [MeV]	$440^{+230+110}_{-200-240}$	191^{+66+25}_{-49-17}	97^{+40+29}_{-29-26}

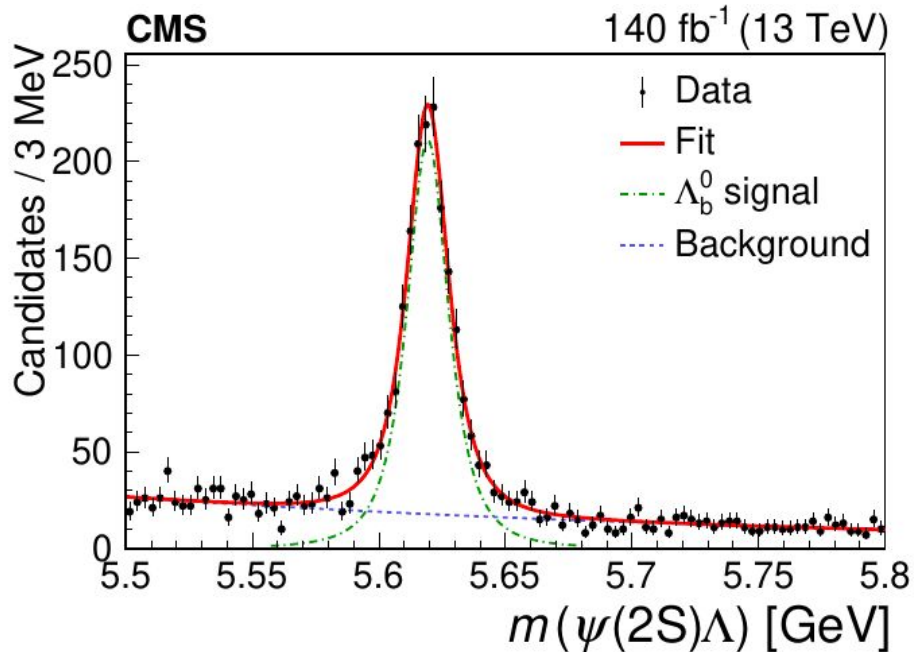
Two new structures, tentatively named **X(6600)** and **X(7300)**, are found, and the **X(6900)** structure observed by LHCb is confirmed. The local significances of these peaks are, for increasing mass, **6.5, 9.4, and 4.1 standard deviations**. Adding interference terms between the three signals results in better agreement to the data in the regions between the resonances and results in shifts of the resonance parameters.

arXiv:2401.16303v1,
CMS-BPH-22-002 ; CERN-EP-2024-006
Submitted to EPJC

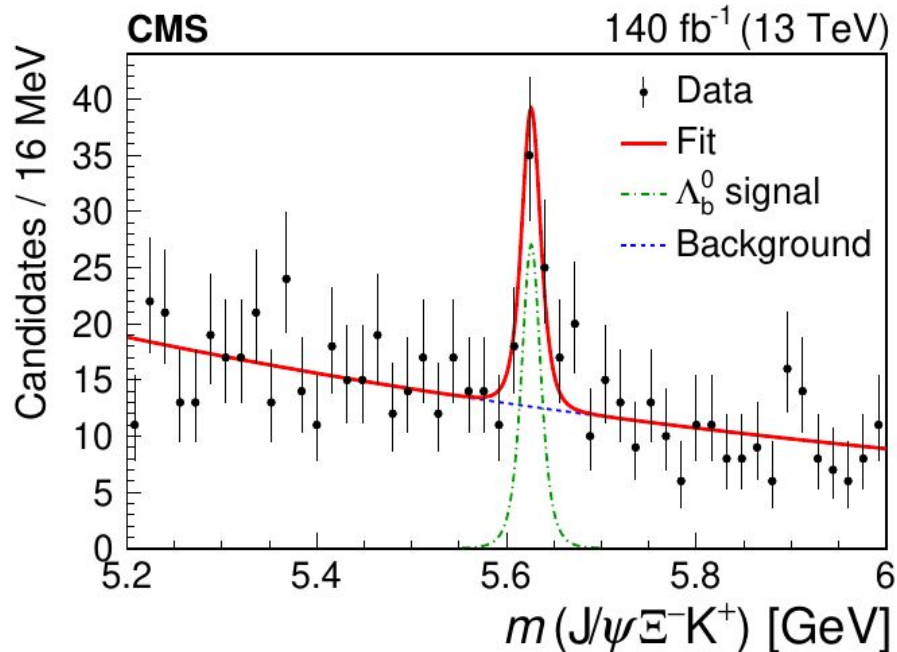
Observation of the $\Lambda_b^0 \rightarrow J/\psi \Xi^- K^+$ decay

Up to now, the hidden-charm pentaquark candidates have been reported only in $J/\psi p$ and $J/\psi \Lambda$ systems. Investigation of other channels with heavier baryons in the decay products, such as Ξ^- and Ω^- , could unveil the existence of doubly or triply strange pentaquarks.

Measured $\psi(2S)\Lambda$ and $J/\psi\Xi^-K^+$ invariant mass distributions



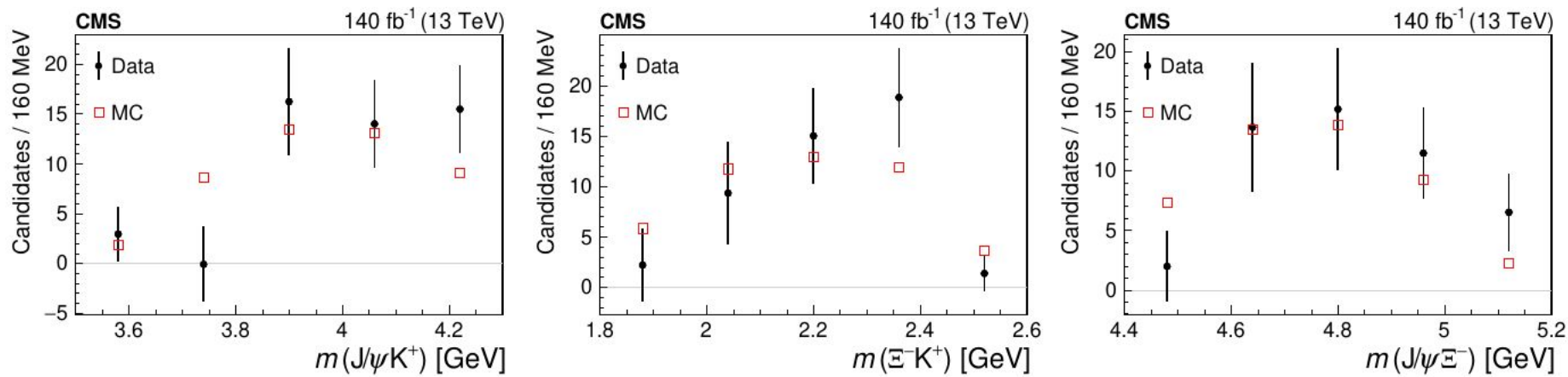
$$N(\Lambda_b^0 \rightarrow \psi(2S)\Lambda) = 1744 \pm 63$$



$$N(\Lambda_b^0 \rightarrow J/\psi\Xi^-K^+) = 46 \pm 11$$

Signal significance is found to be 5.8 standard deviations

Intermediate invariant mass distributions of the $\Lambda_b^0 \rightarrow J/\psi \Xi^- K^+$



The filled circles and empty squares show the measured background-subtracted distributions and the results from the simulation with a phase-space model, respectively.

Branching fraction ratio measurement

$$\mathcal{R} \equiv \frac{\mathcal{B}(\Lambda_b^0 \rightarrow J/\psi \Xi^- K^+)}{\mathcal{B}(\Lambda_b^0 \rightarrow \psi(2S) \Lambda)} = \frac{N(\Lambda_b^0 \rightarrow J/\psi \Xi^- K^+)}{N(\Lambda_b^0 \rightarrow \psi(2S) \Lambda)} \frac{\epsilon_{\psi(2S)\Lambda}}{\epsilon_{J/\psi \Xi^- K^+}} \frac{\mathcal{B}(\psi(2S) \rightarrow J/\psi \pi^+ \pi^-)}{\mathcal{B}(\Xi^- \rightarrow \Lambda \pi^-)}$$

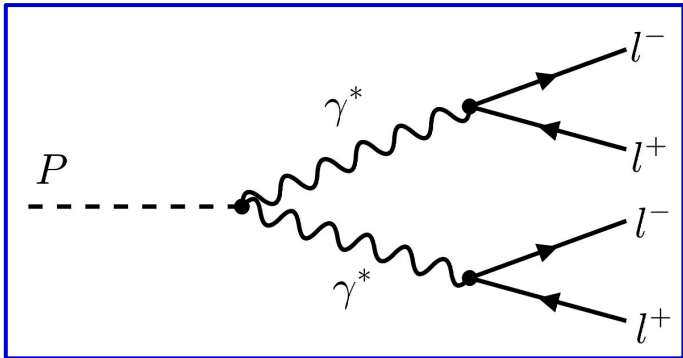
$$\mathcal{R} \equiv \frac{\mathcal{B}(\Lambda_b^0 \rightarrow J/\psi \Xi^- K^+)}{\mathcal{B}(\Lambda_b^0 \rightarrow \psi(2S) \Lambda)} = [3.38 \pm 1.02 \text{ (stat)} \pm 0.61 \text{ (syst)} \pm 0.03 \text{ (}\mathcal{B}\text{)}]\%$$

In summary

- The $\Lambda_b^0 \rightarrow J/\psi \Xi^- K^+$ decay is observed with a significance exceeding 5 standard deviations.
- The distributions of intermediate invariant masses are also presented.
- This is the first discovered multibody decay containing the $J/\psi \Xi^-$ system.

arXiv:2305.04904,
CMS-BPH-22-003 ; CERN-EP-2023-071
Phys. Rev. Lett. 131, 091903

Observation of the rare decay of the η meson to four muons



Observing these rare decays is important because :

- They can serve as precision tests of the standard model.
- They offer sensitivity to different new physics scenarios.
- The interaction between pseudoscalars and photons contributes to the hadronic light-by-light component of the anomalous magnetic moment of the muon.

“Data scouting”

Standard dimuon triggers:

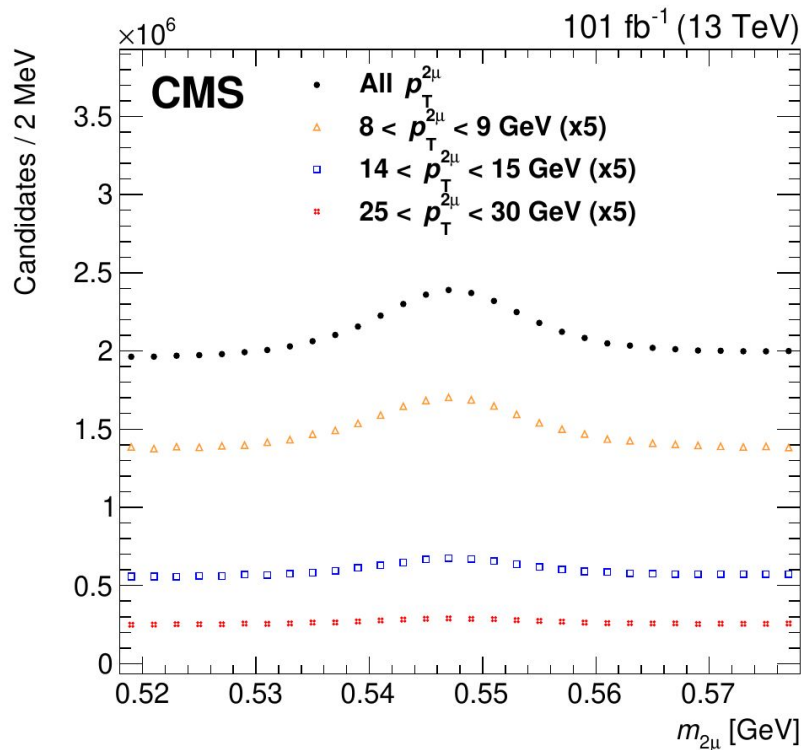
- The HLT processes events at an output rate of about **1 kHz with approximately 1 MB.**
- pT Tthresholds
 - ◆ $p_T(\mu_1) > 15 \text{ GeV}, p_T(\mu_2) > 7 \text{ GeV}$ [2018]
 - ◆ $p_T(\mu_1) > 12 \text{ GeV}, p_T(\mu_2) > 5 \text{ GeV}$ [2017]
- For dimuon resonance masses below about **40 GeV**, the performance of the standard muon triggers deteriorates

Dedicated set of high-rate dimuon triggers:

- Considerably lower muon pT threshold (see table)
- **But, store only a limited amount of information per event**
 - only muons reconstructed at the HLT
 - limited event-level information
- Event size of around 4 kB in 2017 and 8 kB in 2018

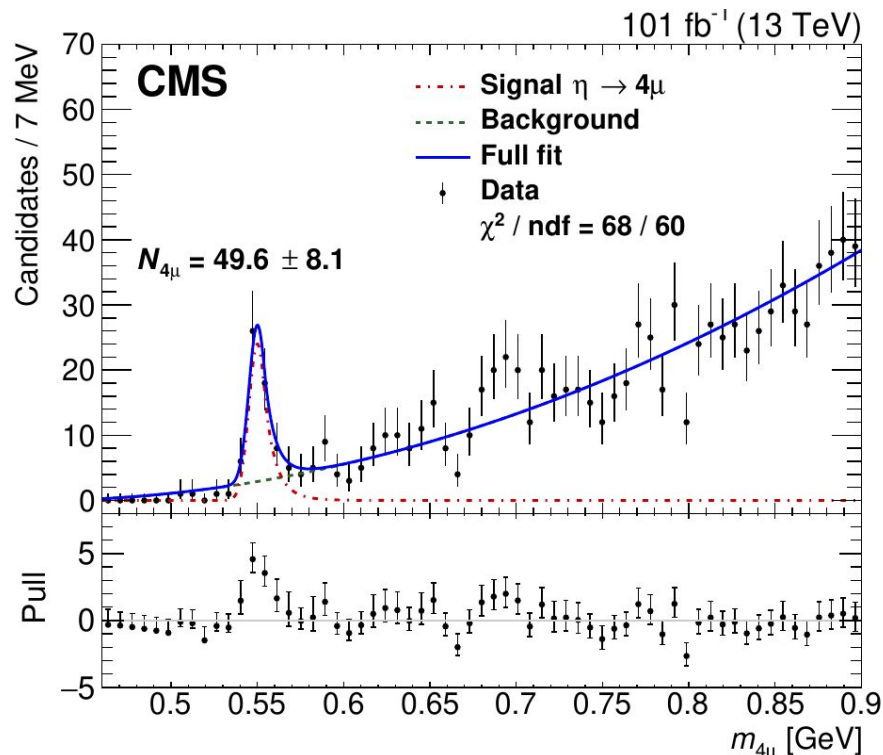
L1 path	p_T [GeV]	$ \eta $	ΔR	$m_{2\mu}$ [GeV]	Charge	Fraction
#1	>4.0 (4.5)	—	<1.2	—	OS	90%
#2	—	< 1.5	< 1.4	—	OS	48%
#3	>15, >7	—	—	—	—	46%
#4	>4.5	< 2.0	—	7–18	OS	9%

Invariant mass spectrum



4.5 million $\eta \rightarrow 2\mu$ decays

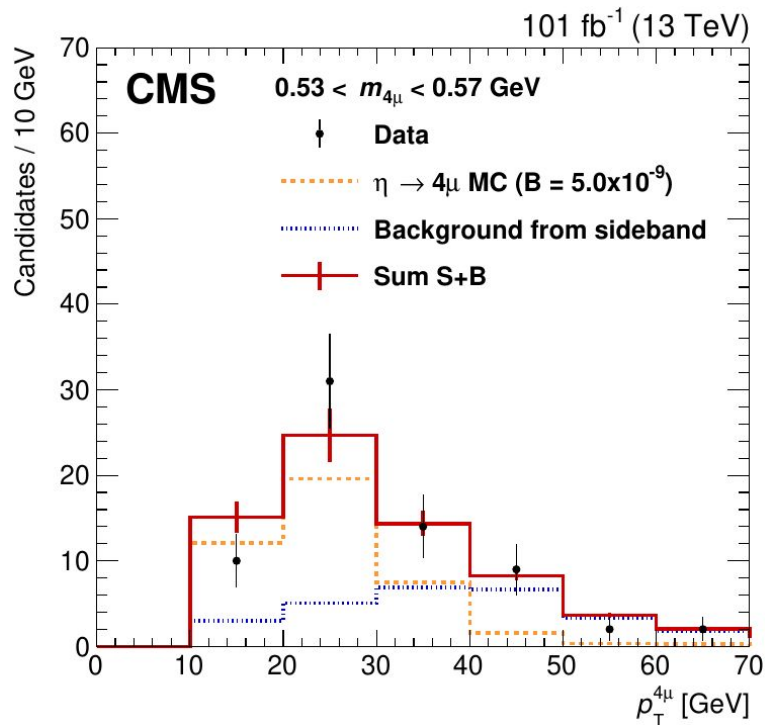
number of events in the selected pT ranges multiplied by five for better visibility.



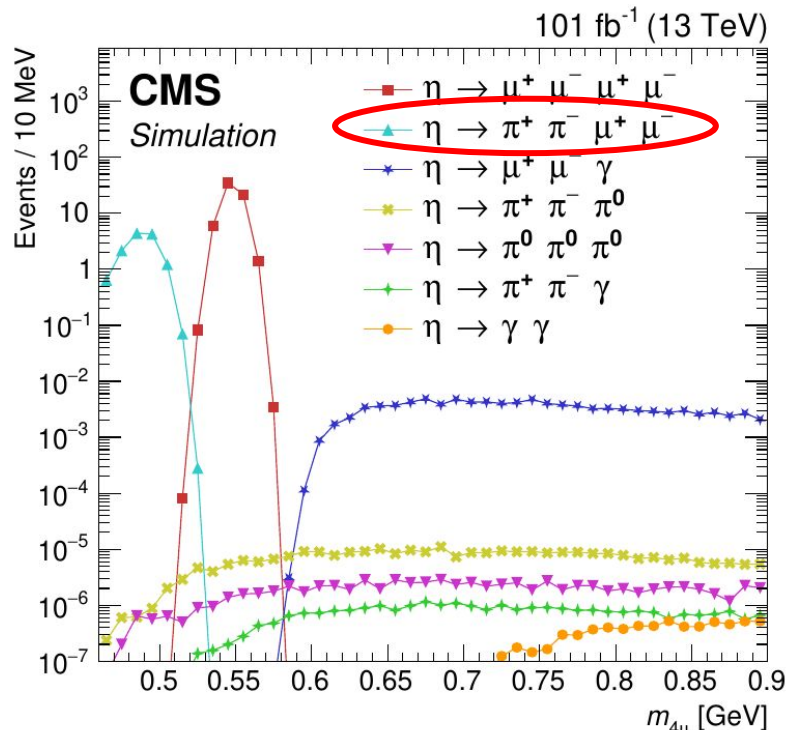
Signal = 49.6 ± 8.1 , background 16.6 ± 0.6

Significance in excess of 5 standard deviations

Checks: p_T spectrum and background contributions



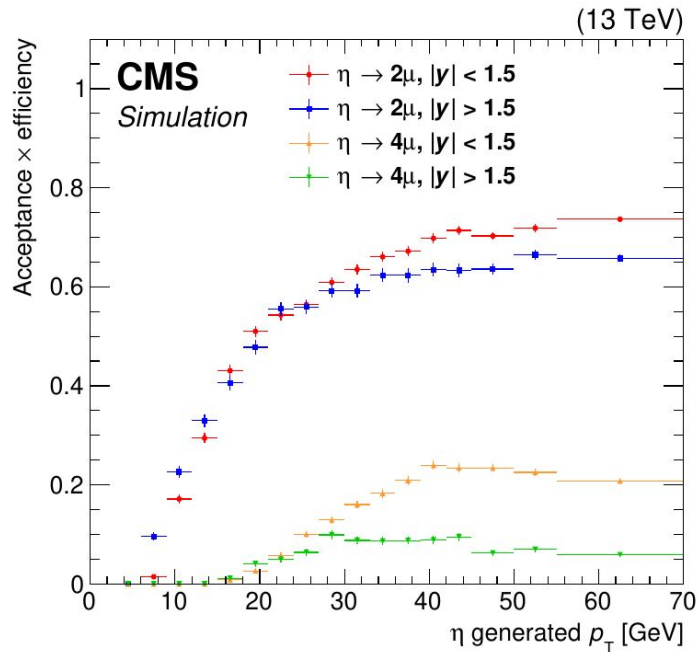
The signal $p_T^{4\mu}$ distribution reweighted based p_T differential production rate measured with the two-muon channel.



Shifts the invariant mass peak (never been observed).

Other decay modes of the η meson provide a negligible contribution.

The branching fraction



The total efficiencies for the four-muon (red and blue points) and two-muon (orange and green points), evaluated through MC simulation

$$\frac{\mathcal{B}_{4\mu}}{\mathcal{B}_{2\mu}} = \frac{N_{4\mu}}{\sum_{i,j} N_{2\mu}^{i,j} \frac{A_{4\mu}^{i,j}}{A_{2\mu}^{i,j}}}$$

32 bins in p_T in the range 7–70 GeV and two bins in $|y|$

$$\frac{\mathcal{B}_{4\mu}}{\mathcal{B}_{2\mu}} = [0.86 \pm 0.14(\text{stat}) \pm 0.12(\text{syst})] \times 10^{-3}$$

$$\mathcal{B}(\eta \rightarrow 4\mu) = [5.0 \pm 0.8(\text{stat}) \pm 0.7(\text{syst}) \pm 0.7(\mathcal{B}_{2\mu})] \times 10^{-9}$$

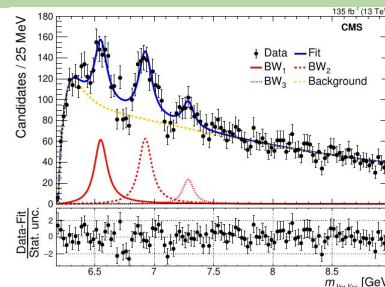
In summary,

- The first observation of the η meson's rare double-Dalitz decay to four muons is reported.
- This result is in agreement with theoretical predictions.
- With high-rate triggers in future will enable a detailed study of doubly virtual pseudoscalar transition form factors (TFF's)

Summary

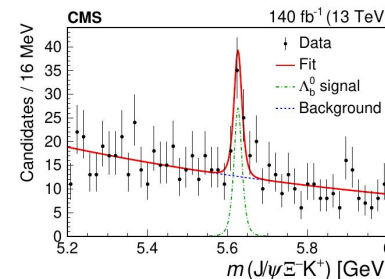
Observation of new structure in the $J/\psi J/\psi$ mass spectrum

Two new structures, tentatively named $X(6600)$ and $X(7300)$, are found, and the $X(6900)$ structure observed by LHCb is confirmed



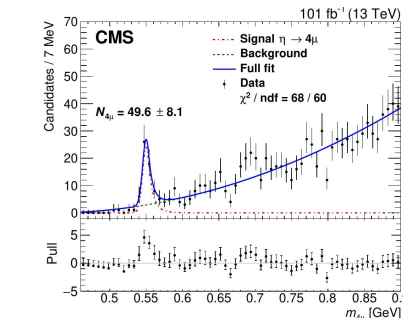
Observation of the $\Lambda_b^0 \rightarrow J/\psi \Xi^- K^+$ decay

This is the first discovered multibody decay containing the $J/\psi \Xi^-$ system.



Observation of the rare decay of the η meson to four muons

With high-rate triggers in future will enable a detailed study of doubly virtual pseudoscalar transition form factors (TFF's)



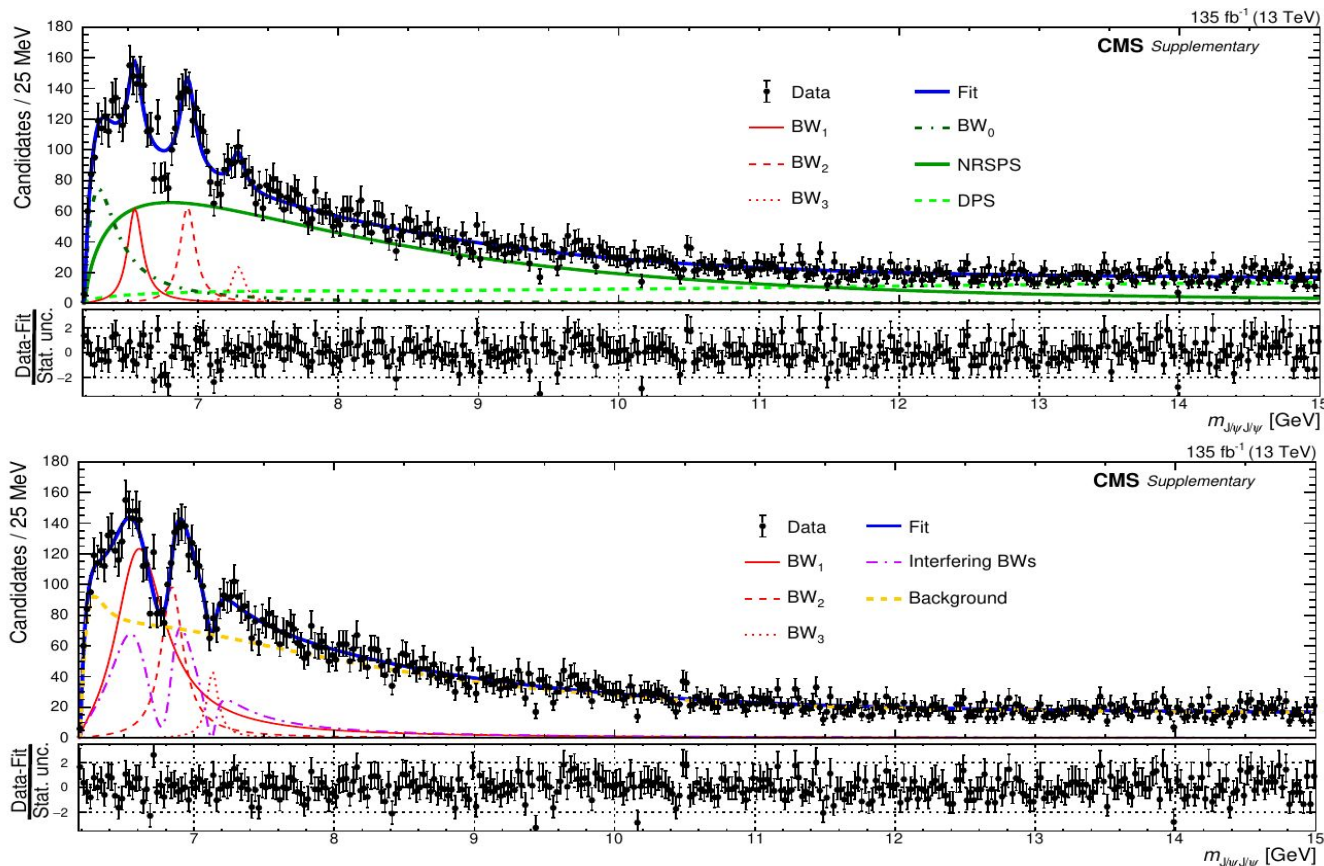
The new results are important for understanding the strong interaction processes in hadronic decays.

THANKS for listening!



Backup slides

The $J/\psi J/\psi$ invariant mass spectrum in the range up to 15 GeV

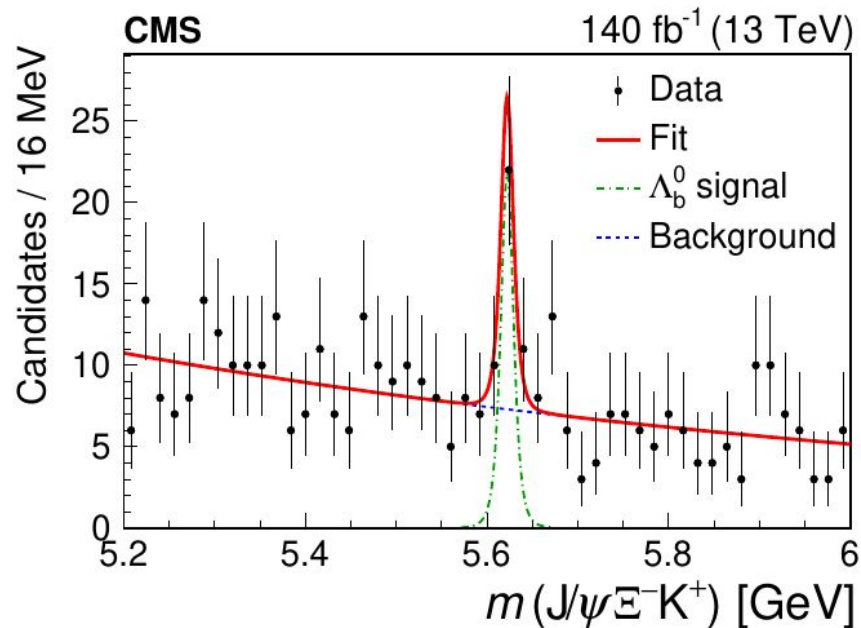
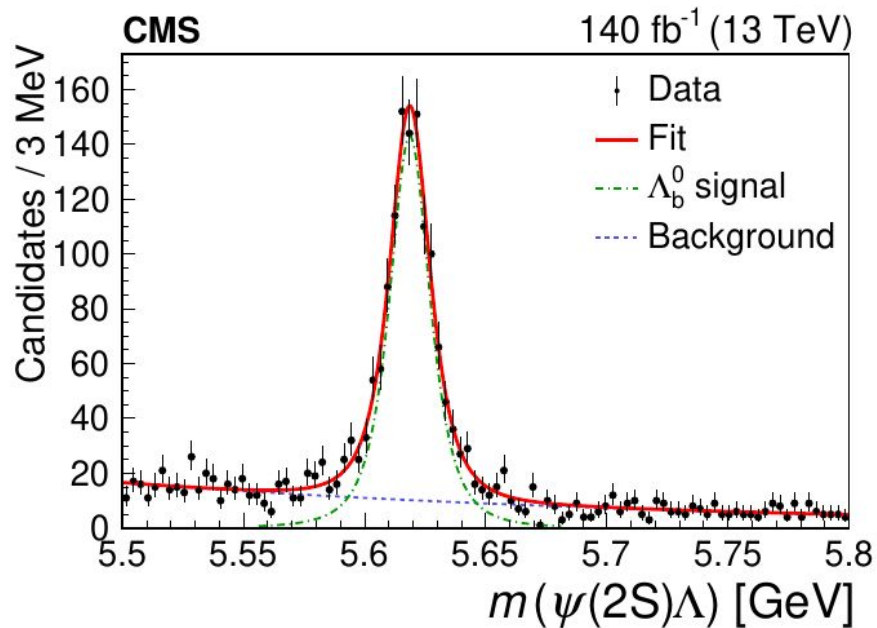


The $J/\psi J/\psi$ invariant mass spectrum with the no-interference fit (upper) and the interference fit (lower) in the full fit range. The "Interference BWs" curve is the total contribution of all the interference amplitudes and their cross terms. The lower portion of the plots shows the pulls, i.e., the number of standard deviations (statistical uncertainties only) that the binned data differ from the fit.

Optimized selection criteria for the signal decay mode $\Lambda_b^0 \rightarrow J/\psi \Xi^- K^+$

Variable	Selection
$ m(p\pi^-) - m_{\text{PDG}}(\Lambda) $	$< 8 \text{ MeV}$
$ m(\Lambda\pi^-) - m_{\text{PDG}}(\Xi^-) $	$< 6 \text{ MeV}$
$p_T(\Lambda_b^0)$	$> 11.5 \text{ GeV}$
$p_T(J/\psi)$	$> 6.5 \text{ GeV}$
$p_T(\Xi^-)$	$> 2.6 \text{ GeV}$
$p_T(\Lambda)$	$> 2.2 \text{ GeV}$
$p_T(K^+)$	$> 1.2 \text{ GeV}$
$\mu^+\mu^-\Xi^-K^+$ vertex fit probability	$> 5\%$
$\Lambda\pi^-$ vertex fit probability	$> 5\%$
$p\pi^-$ vertex fit probability	$> 1\%$
Ξ^- vertex displacement from Λ_b^0 vertex	$> 3 \text{ s.d.}$
Λ vertex displacement from Ξ^- vertex	$> 0 \text{ s.d.}$
Λ_b^0 vertex displacement from PV	$> 3 \text{ s.d.}$
Angle between Ξ^- momentum and displacement	$< 0.0447 \text{ rad}$
Angle between Λ momentum and displacement	$< 0.14 \text{ rad}$
Angle between Λ_b^0 momentum and displacement	$< 0.0447 \text{ rad}$
PV impact parameter for pion from Ξ^- decay	$> 0.4 \text{ s.d.}$
PV impact parameter for kaon	$> 0.4 \text{ s.d.}$

Measured $\psi(2S)\Lambda$ and $J/\psi\Xi^-K^+$ invariant mass distributions



Corresponding fits used for the measurement of R.

The relative systematic uncertainties in the measurement of R.

Source	Uncertainty (%)
Tracking efficiency	2.3
$p_T(\Lambda_b^0)$ spectrum	4.7
Signal model	3.9
Background model	6.7
Non- ψ (2S) contribution	2.5
Limited size of MC samples	5.6
Selection efficiency	14.3
Total	18.2